Stem Cell Reports
Article

ISSCR

OPEN ACCESS

Accelerated mitochondrial dynamics promote spermatogonial differentiation

Zhaoran Zhang,[1,2] Junru Miao,[1,2] Hanben Wang,[1] Izza Ali,[1] Duong Nguyen,[1] Wei Chen,[1] and Yuan Wang[1,3,*]
[1]Department of Animal Sciences, College of Agriculture and Natural Resources, Michigan State University, East Lansing, MI 48824, USA
[2]These authors contributed equally
[3]Lead contact
*Correspondence: wangyu81@msu.edu
https://doi.org/10.1016/j.stemcr.2024.09.006

SUMMARY

At different stages of spermatogenesis, germ cell mitochondria differ remarkably in morphology, architecture, and functions. However, it remains elusive how mitochondria change their features during spermatogonial differentiation, which in turn impacts spermatogonial stem cell fate decision. In this study, we observed that mitochondrial fusion and fission were both upregulated during spermatogonial differentiation. As a result, the mitochondrial morphology remained unaltered. Enhanced mitochondrial fusion and fission promoted spermatogonial differentiation, while the deficiency in DRP1-mediated fission led to a stage-specific blockage of spermatogenesis at differentiating spermatogonia. Our data further revealed that increased expression of pro-fusion factor MFN1 upregulated mitochondrial metabolism, whereas DRP1 specifically regulated mitochondrial permeability transition pore opening in differentiating spermatogonia. Taken together, our findings unveil how proper spermatogonial differentiation is precisely controlled by concurrently accelerated and properly balanced mitochondrial fusion and fission in a germ cell stage-specific manner, thereby providing critical insights about mitochondrial contribution to stem cell fate decision.

INTRODUCTION

Sustainable production of functional sperm is essential for maintaining proper male fertility (Mecklenburg and Hermann, 2016). Spermatogonial stem cells (SSCs), a rare subset of undifferentiated spermatogonia, are the foundation of continuous sperm production during spermatogenesis (Mecklenburg and Hermann, 2016). Like other tissue stem cells, SSCs can undergo both self-renewal and differentiation. They maintain a pool of undifferentiated spermatogonia and the subsequent progenitor spermatogonia that are poised for differentiation. Extrinsic factors such as glial cell-derived neurotrophic factor and fibroblast growth factor 2 are required for maintaining SSC self-renewal, while signaling molecules such as retinoic acid (RA) drive undifferentiated spermatogonia toward differentiation (Kubota et al., 2004; Masaki et al., 2018). CD90 and CD9 surface antigens are often used to enrich undifferentiated spermatogonia and SSCs which express marker genes, such as *Gfrα1*, *Id4*, and *Plzf*, at high levels (Buaas et al., 2004; Chan et al., 2014; Kanatsu-Shinohara et al., 2004). In contrast, *Kit* and *Stra8* are highly expressed in differentiating spermatogonia and early-stage spermatocytes (Anderson et al., 2008; Mecklenburg and Hermann, 2016). A balanced SSC self-renewal and irreversible spermatogonial differentiation are the key to maintaining the stem cell pool while producing millions of sperm daily for sustainable male fertility.

Mammalian SSCs and spermatogonia are located at the base of seminiferous tubules in the testis. However, it has been implicated that SSCs reside in an avascular hypoxic environment while progenitors and differentiating spermatogonia preferentially locate adjacent to the interstitial space where they have an easier access to oxygen (Chan et al., 2014; Lord and Nixon, 2020). This differential oxygen availability indicates distinct metabolic preferences between SSCs and differentiating spermatogonia. Indeed, published reports have revealed that metabolism plays critical roles in maintaining the balance between SSC self-renewal and spermatogonial differentiation (Chen et al., 2020a; Helsel et al., 2017; Kanatsu-Shinohara et al., 2016). SSCs and undifferentiated spermatogonia possess a higher glycolytic capacity and prefer a low oxygen tension environment (Helsel et al., 2017; Kanatsu-Shinohara et al., 2016). Upon differentiation, spermatogonia shift toward the more efficient aerobic mitochondrial respiration in response to increased metabolic demands, accompanied by an upregulated reactive oxygen species (ROS) level (Chen et al., 2020a). Consistently, the inhibition of mitochondrial respiration blocks spermatogonial differentiation (Chen et al., 2020a), thereby supporting the notion that a metabolic shift from glycolysis to mitochondrial respiration is required for spermatogonial differentiation. These findings align with several transcriptome studies, revealing that glycolytic enzymes and hypoxia-responsive factors are highly expressed in human and mouse SSCs, while regulators reflecting mitochondrial biogenesis, activities, and oxidative phosphorylation (OXPHOS) are upregulated in differentiating spermatogonial progenitors (Guo et al., 2017; Hermann et al., 2018; Lord and Nixon, 2020).

Mitochondrial metabolism contributes to multiple biological processes such as cell signaling, stem cell differentiation, and lineage commitment, well beyond its canonical

role in energy production. Metabolites generated through the mitochondrial tricarboxylic acid (TCA) cycle may serve as enzymatic cofactors for epigenetic regulation (Cai et al., 2011). For example, acetyl-coenzyme A (CoA) from the TCA cycle provides the acetyl group to histone acetyltransferases for histone acetylation, while α-ketoglutarate serves as cofactors for Ten Eleven Translocation family members and Jumonji histone demethylases in demethylation of DNA and histones (Klose et al., 2006). ROS from OXPHOS may also alter protein stability and function via oxidative protein modification or act as a secondary messenger to trigger signaling cascades (Chandel et al., 1998; Lo Conte and Carroll, 2013). It has been reported that mitochondrial features differ significantly between neural stem cells (NSCs) and committed progenitors, and disrupting mitochondrial activities specifically impairs NSC self-renewal via ROS-NRF2-mediated retrograde (mitochondria to the nucleus) signaling without disturbing ATP generation (Khacho et al., 2016). Thus, mitochondria not only provide bioenergy but also may alter the levels of active metabolites and ROS in a cell type-dependent manner, which in turn impacts gene transcription, protein activity, and cell fate decision.

Mitochondrial metabolism is not only regulated by mitochondrial enzyme levels but also affected by mitochondrial features and activities. Mitochondria are highly dynamic organelles that undergo coordinated cycles of fusion and fission, which are collectively known as mitochondrial dynamics, to maintain their proper morphology, distribution, metabolism, and function (Chan, 2006). Mitochondrial fusion (mitofusion) is mainly regulated by two GTPases, Mitofusin 1 (MFN1) and Mitofusin 2 (MFN2), at the outer mitochondrial membrane (Chan, 2006; Eura et al., 2003), as well as by Optic Atrophy 1 (OPA1) GTPase at the inner mitochondrial membrane (Alexander et al., 2000). By contrast, GTPase dynamin-related protein 1 (DRP1, also called DMN1L) and several mitochondrial DRP1 adaptors (e.g., Mitochondrial Fission 1/FIS1 and Mitochondrial Fission Factor/MFF) play essential roles in mediating mitochondrial fission (Chan, 2006). Our previous study demonstrated that both MFN1 and MFN2 are essential for proper germ cell development (Chen et al., 2020b; Zhang et al., 2016). Conditional deletion of either *Mfn1* or *Mfn2* in germ cells led to a stage-specific blockage of spermatogenesis at differentiating spermatogonia, supporting a critical requirement of mitofusion in spermatogonial differentiation. In *Drosophila*, *Drp1* inhibition led to a loss of germline stem cells and spermatogonia due to ROS accumulation and epidermal growth factor receptor activation in adjacent somatic cells (Sênos Demarco and Jones, 2019). In addition, several studies suggest that defects of mitochondrial fission severely jeopardize late spermatogenesis. For example, conditional knockout of *Fis1*, a DRP1 adaptor, by a germ cell-specific driver, *Stra8-Cre*, resulted in early spermatid arrest with giant multinucleated cells containing dysfunctional mitochondria and defects in mitophagy (Varuzhanyan et al., 2021a). Mice with deletion of *Mff*, another DRP1 adaptor, also had reduced fertility and sperm count (Varuzhanyan et al., 2021b). The remaining sperm in *Mff* mutants displayed aberrant morphology and motility with decreased respiratory chain complex IV activity. The role of mitochondrial fission in mammalian spermatogonial formation however remains to be characterized; moreover, it is unclear how mitochondrial dynamics impact the balance of SSC self-renewal and spermatogonial differentiation. In this study, we examined the functions of mitochondrial dynamics in undifferentiated and differentiating spermatogonia. We found that regulators for mitochondrial fusion and fission were upregulated in differentiating spermatogonia. Enhanced mitochondrial dynamics promoted spermatogonial differentiation, while conditional *Drp1* deletion from germ cells blocked spermatogenesis at the differentiating spermatogonial stage. Our data further revealed the specific functional mechanisms employed by different mitochondrial dynamics players in regulating spermatogonial differentiation.

RESULTS

Mitochondrial dynamics are accelerated in differentiating spermatogonia

In our previous study, we demonstrated that a bioenergetic shift from glycolysis to mitochondrial respiration is required for spermatogonial differentiation (Chen et al., 2020a). In alignment with our data, published transcriptome studies revealed that glycolytic enzymes were downregulated (Guo et al., 2017; Hermann et al., 2018). By contrast, the regulators in mitochondrial functions were increased, including MFN1 and MFN2, two GTPases that promote mitofusion, suggesting that mitofusion was accelerated. Because elevated mitofusion leads to elongated tubular mitochondria that favor OXPHOS, a prevailing model is that mitofusion needs to be increased during spermatogonial differentiation to support upregulated mitochondrial respiration and energy demand from differentiating spermatogonia (Lord and Nixon, 2020; Zhang et al., 2022). To test this model, we examined mitochondrial morphology and mitochondrial DNA (mtDNA) copy number of undifferentiated and differentiating spermatogonia. For *in vitro*-cultured spermatogonia, we first confirmed that undifferentiated mCherry+ spermatogonia were able to reconstitute spermatogenesis in $Kit^{w/w\text{-}v}$ mice, a commonly used transplantation recipient that lacks endogenous germ cells (Figure S1A, the right panel) (Ogawa et al., 2000). In

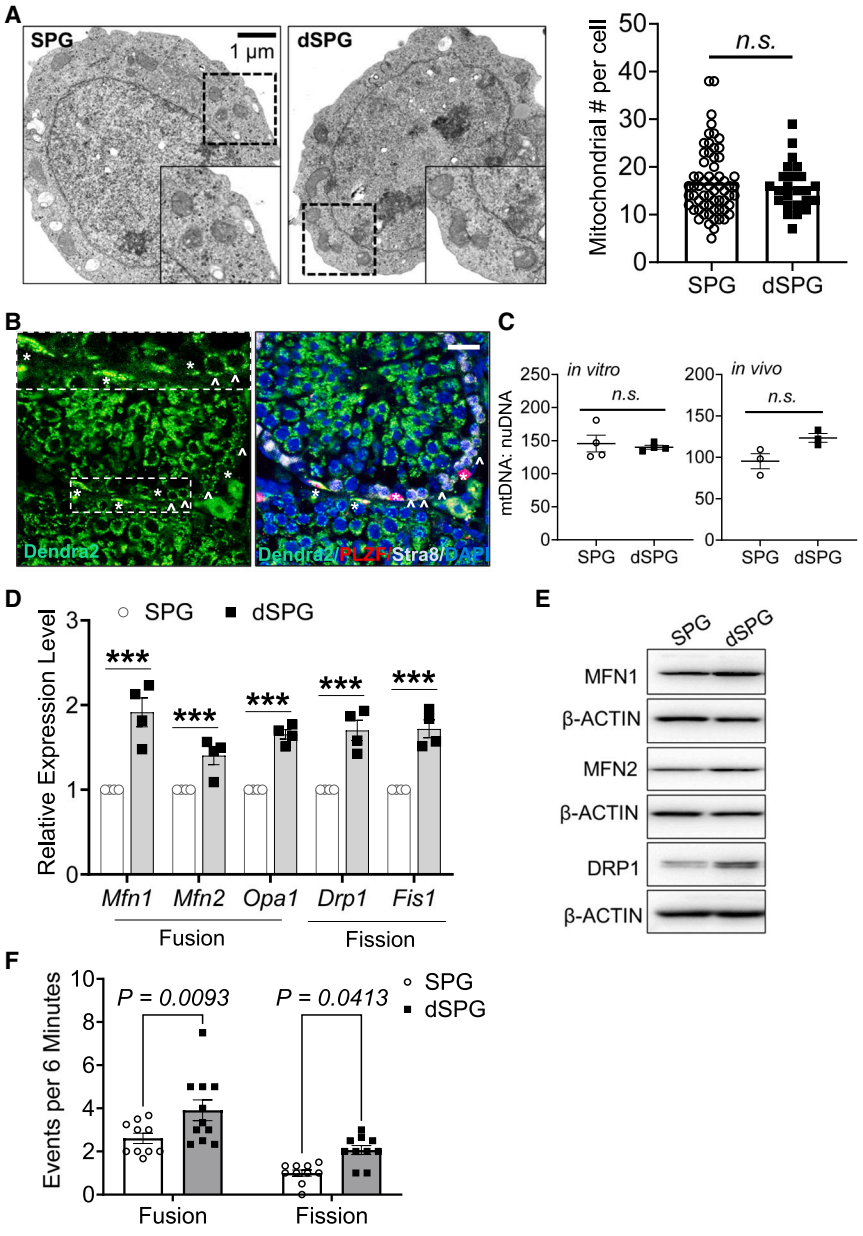

Figure 1. Mitochondrial dynamics were upregulated during spermatogonial differentiation

(A) Mitochondrial architecture was not altered in undifferentiated (SPG) vs. RA-induced differentiating spermatogonia (dSPG), as examined by TEM and mitochondrial number per cell (the right panel) calculated from more than 24 cells per group.

(B) IHF staining was performed on testes expressing mitochondrion-localized Dendra2 GFP from 4-week mice with antibodies against PLZF (red) and STRA8 (gray), counterstained with the nuclear dye DAPI. Scale bar: 20 μm. The insert shows a blow-up image of a representative region. Mitochondrial signals were not obviously altered in PLZF+ SPG vs. RA-induced dSPG.

(C) The mtDNA copy number was not significantly altered in cultured SPG vs. dSPG (the left panel) or in CD9+/KIT− SPG vs. KIT+ dSPG from P12 mouse testes sorted by flow cytometry (the right panel), as measured by real-time PCR. *Pecam*, a nuclear DNA-coded gene, was used as the single-copy control. $n = 3$.

(D and E) The transcript levels measured by real-time RT-PCR (D) and protein expression determined by western blots (E). Mitochondrial dynamics regulators were upregulated in RA-induced dSPG, compared to those of SPG. $n = 4$; ***: $p < 0.001$.

(F) Increased mitochondrial fusion and fission during spermatogonial differentiation were detected by confocal microscopy. *PhAM; Ddx4-Cre* spermatogonia were induced to differentiate by RA, and the 3D mitochondrial images in live cells were acquired for 6 min. The events of fusion and fission were quantified by changes of mitochondrial volume over time. $n = 10$. (A, C, E–F) Data are presented as mean ± SEM, *n.s.*, no statistical significance.

addition, upon induction of RA, the CD9+ undifferentiated spermatogonia readily became KIT+ differentiating spermatogonia (Figure S1A, the left panel). Genes that mark SSCs (*Plzf* and *Gfrα1*) were highly expressed in these cultured spermatogonia and downregulated upon RA-induced differentiation, while the genes that indicate differentiation (*Kit* and *Stra8*) were upregulated in KIT+ differentiating spermatogonia (Figure S1B). Consistent with published findings (Chen et al., 2020a; Guo et al., 2017; Hermann et al., 2018), levels of ROS and enzymes in mitochondrial respiration were elevated upon differentiation (Figures S1C–S1E).

To our surprise, no significant difference was observed via transmission electron microscopy (TEM) in mitochondrial morphology and number between undifferentiated spermatogonia and differentiating spermatogonia induced by RA treatment (Figure 1A). We further performed immunohistofluorescent (IHF) assays to examine mitochondrial morphology with a *PhAM; Ddx4-Cre* mouse model that expresses a mitochondrion-localized Dendra2 green fluorescent protein in all germ cells from embryonic day 15.5 upon the excision of a floxed stop segment by CRE recombinase under a germ cell-specific *Ddx4* promoter (Gallardo et al., 2007; Pham et al., 2012). We found that

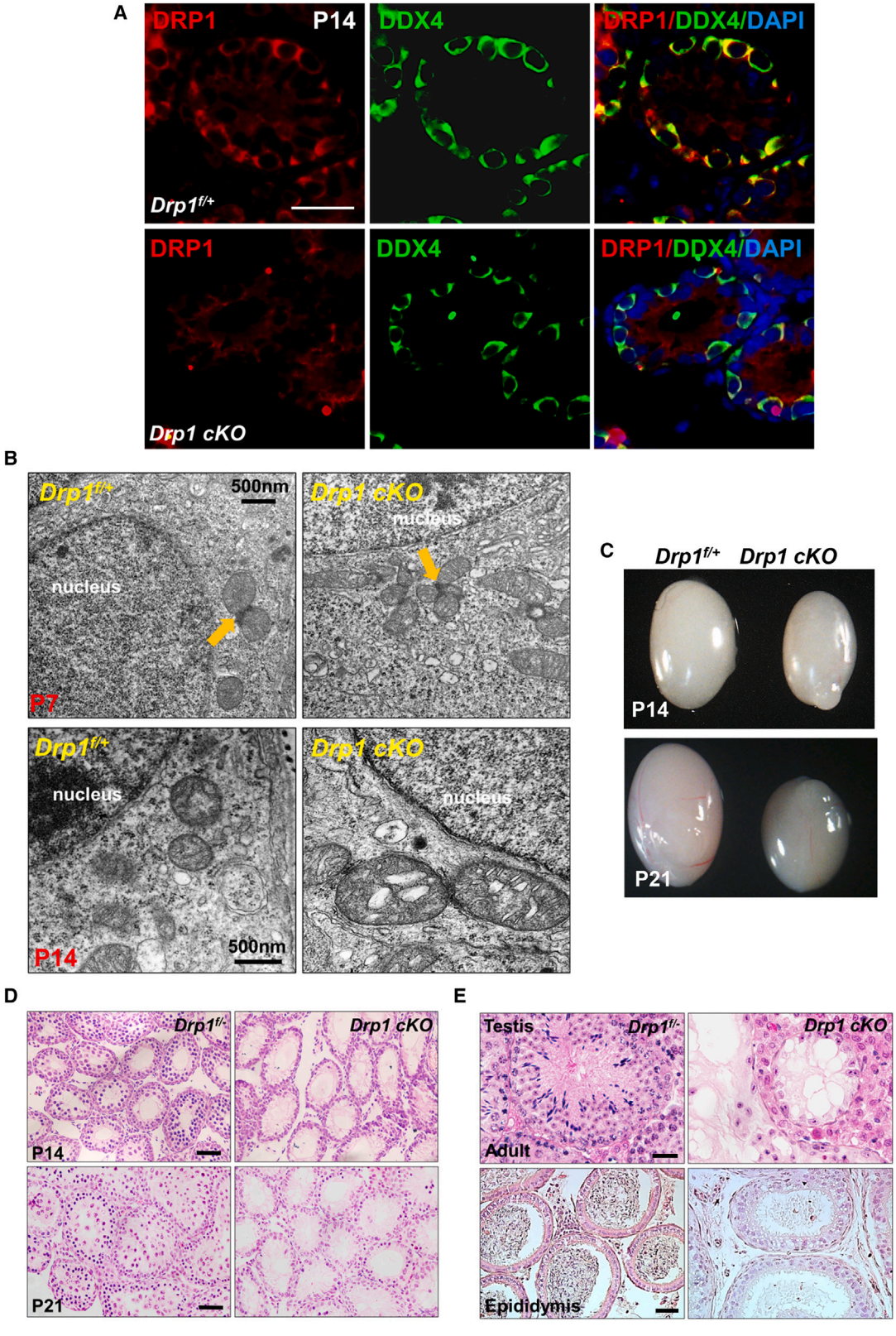

(legend on next page)

spermatocytes in the middle of seminiferous tubule exhibited much higher mitochondrial signals than spermatogonia at the basal compartment. PLZF+ undifferentiated spermatogonia displayed similar mitochondrial fluorescence to that of STRA8+ differentiating spermatogonia (Figure 1B). The mtDNA copy number between undifferentiated and RA-induced differentiating spermatogonia (Figure 1C, left panel) was also comparable. Likewise, we did not find obvious difference in mtDNA copy number between CD9+/KIT-undifferentiated spermatogonia and KIT+ differentiating cells that were directly collected from testes (Figure 1C, right panel).

To explore the mechanism underlying these phenomena, we examined the expression of regulators of both mitochondrial fusion and fission. Interestingly, we found that the transcript levels of key regulators in mitochondrial fusion (MFN1, MFN2, and OPA1) and fission (DRP1, FIS1, and MFF) were upregulated upon RA induction (Figure 1D). Consistently, their protein levels were also increased in differentiating spermatogonia collected from *in vitro*-cultured germ cells or from testes, compared to undifferentiated spermatogonia (Figures 1E and S2; Table S1), suggesting fusion and fission were both accelerated upon spermatogonial differentiation.

To confirm the accelerated mitochondrial dynamics upon spermatogonial differentiation, we established spermatogonial culture from *PhAM; Ddx4-Cre* mice to track the mitochondrial activities in real time by confocal microscopy. We acquired high-resolution 3D images over time in live spermatogonia and deconvolved these images to calculate the occurrence of mitochondrial fusion and fission based on the changes of mitochondrial volume. We found that both fusion and fission were indeed increased during RA-induced spermatogonial differentiation (Figure 1F).

Drp1 deficiency in germ cells leads to male infertility

It has been reported that conditional knockout of *Mfn1* or *Mfn2* from germ cells leads to a stage-specific block of spermatogenesis at differentiating spermatogonia (Chen et al., 2020b; Zhang et al., 2016). To understand whether mitochondrial fission is also required for spermatogonial differentiation, we generated germ cell-specific conditional knockout of *Drp1*, the key GTPase for mitochondrial fission (Figure S3A), via a *Ddx4-Cre* driver, in which CRE recombinase under a *Ddx4* promoter specifically deletes *Drp1* in all germ cells from embryonic day 15.5 (Gallardo et al., 2007). We confirmed that no DRP1 protein was detected in DDX4+ germ cells from *Drp1* conditional knockout (i.e., $Drp1^{f/-}$*; Ddx4-Cre*, abbreviated as *Drp1 cKO*) mice (Figure 2A). We further examined the mitochondrial morphology and architecture by TEM. In spermatogonia and early-stage spermatocytes, electron-dense granules, known as intermitochondrial cement (IMC) containing clustered mitochondria with RNA-binding proteins, have been known for regulating critical germ cell functions. We found that IMC remained intact in spermatogonia from *Drp1 cKO* mice (Figure 2B). However, the mitochondrial morphology started to become heterogeneous in *Drp1 cKO* mice compared to their litter control at post-natal day (P)7 (Figure 2B). Significantly enlarged mitochondria were observed at P14 in *Drp1 cKO* germ cells (Figure 2B), and many contained vacuoles, demonstrating that the mitochondrial fission was blocked due to DRP1 deficiency.

Compared with their littermate controls, *Drp1 cKO* testes were smaller at P14 and were dramatically reduced in size at P21 (Figure 2C). Histological examination showed that spermatogonia remained intact at P7 (Figure S3B), while, at P14 and P21, germ cell formation was significantly reduced in *Drp1 cKO* testes with much fewer spermatocytes (Figure 2D). No elongated spermatids or sperm were detected in either testes or epididymis from *Drp1 cKO* adult mice (Figures 2D and 2E).

Reduced mitochondrial fission blocks spermatogonial differentiation

We further examined the germ cell composition of these *Drp1 cKO* mice by IHF assays with antibodies against DDX4 (pan-germ cells), PLZF (spermatogonia), and SYCP3 (spermatocytes). In *Drp1 cKO* mice at P14 and P21, DDX4+ germ cells were mainly present along the basement membrane of the seminiferous tubules, where PLZF+ spermatogonia were located (Figure 3A). By contrast, DDX4+ spermatocytes were readily detected at the lumen of seminiferous tubules in wild-type littermate controls

Figure 2. Deficiency of mitochondrial fission in germ cells leads to male infertility

(A) The expression of DRP1 protein was not detected in DDX4+ germ cells from P14 mouse *Drp1 cKO* testis, as analyzed by IHF staining with antibodies against DRP1 and DDX4, counterstained with DAPI. Scale bar: 25 μm.

(B) Mitochondrial architecture was examined by TEM on testicular sections from $Drp1^{f/+}$ and *Drp1 cKO* mice at P7 and P14. Orange arrows point to IMC in spermatogonia. Mitochondria were enlarged in *Drp1 cKO* germ cells.

(C) The morphology of control and *Drp1 cKO* testes at P14 and P21. The size of testes was decreased in *Drp1 cKO* mice.

(D) Histological studies on $Drp1^{f/-}$ and *Drp1 cKO* testis from mice at P14 and P21. Germ cells were reduced in *Drp1 cKO* mice. Scale bar: 50 μm.

(E) Histology on $Drp1^{f/-}$ and *Drp1 cKO* testis and epididymis sections from adult mice. No sperm were detected in *Drp1 cKO* mice. Scale bar: 25 μm.

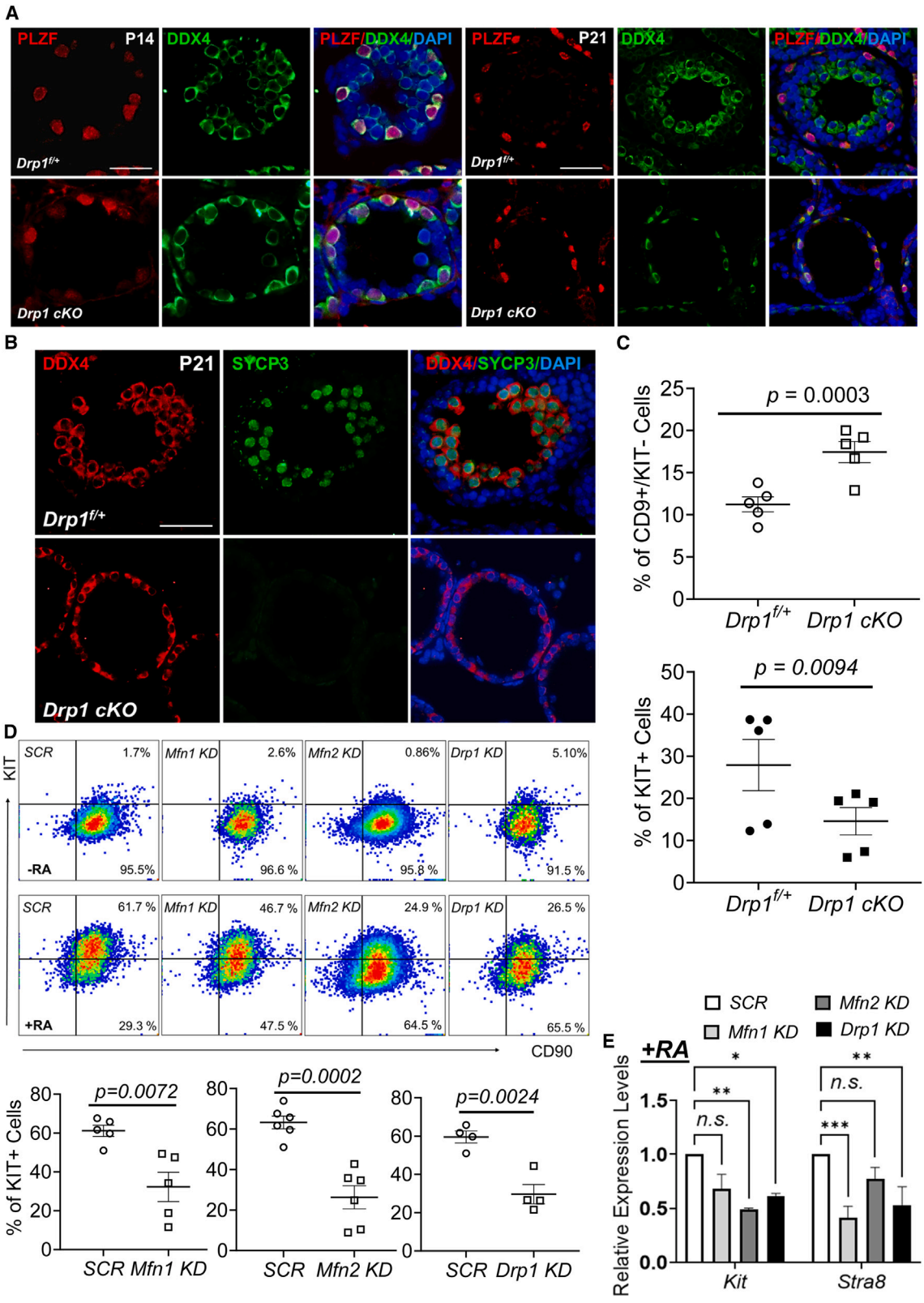

(legend on next page)

(Figure 3A). Few SYCP3+ spermatocytes were detected in *Drp1 cKO* testes (Figure 3B). Interestingly, PLZF+ spermatogonia at the base of the seminiferous epithelium were not obviously affected by *Drp1* deletion from germ cells during early spermatogenesis (Figures 3A, S3C, and S3D). No apparent differences were observed in the number of PLZF+ spermatogonia in *Drp1* cKO vs. littermate controls at P7, P14, and P21 (Figures 3A, S3C, and S3D).

To further determine whether *Drp1* deficiency affects spermatogonial differentiation, we performed flow cytometry analyses on *Drp1 cKO* mice and their littermate controls. We found that the formation of KIT+ differentiating spermatogonia in *Drp1 cKO* testes was decreased, accompanied by an increased percentage of CD9+/KIT− undifferentiated spermatogonia at P14 (Figure 3C). This result was similar to what we had previously observed when the pro-fusion factors *Mfn1* or *Mfn2* were deleted in DDX4+ germ cells (Chen et al., 2020b), demonstrating that deficiency of either mitochondrial fusion or fission will lead to blocked spermatogonial differentiation during spermatogenesis. Notably, the reduction of KIT+ differentiating spermatogonia was unlikely due to increased apoptosis of differentiating spermatogonia. We did not observe any significant alteration in the percentages of Annexin V+/propidium iodide (PI)+ pro-apoptotic or PI+ apoptotic cells upon *Drp1 cKO* (Figure S4A).

The increased CD9+/KIT− undifferentiated spermatogonia in *Drp1 cKO* testes could be caused by blocked spermatogonial differentiation. Alternatively, this may be due to increased spermatogonial proliferation. To distinguish these two possibilities, we examined the effects of disrupted mitochondrial dynamics on spermatogonial proliferation and differentiation by conducting gene knockdown in primarily cultured spermatogonia (Figure S4B). We observed that prolonged downregulation of either MFN1 or DRP1 (>12 days) reduced spermatogonial proliferation, while reduced MFN2 expression increased spermatogonial number over 20-day culture (Figure S4C). More importantly, we found that RA-induced spermatogonial differentiation was significantly reduced by knocking down *Mfn1*, *Mfn2*, or *Drp1* (Figure 3D). Consistently, the genes indicating spermatogonial differentiation, including *Kit* and *Stra8*, were downregulated (Figure 3E). Taken together, our data reveal that properly balanced mitochondrial dynamics is essential for spermatogonial differentiation during spermatogenesis.

Accelerated mitochondrial dynamics promote spermatogonial differentiation

To understand how accelerated mitochondrial dynamics affect spermatogonial development, we enforced the expression of key regulators of mitochondrial fusion (MFN1 and MFN2) or fission (DRP1) in spermatogonia (Figures S5A and S5B). In addition, TEM confirmed that mean mitochondrial area increased in spermatogonia upon overexpression of pro-fusion factors MFN1 or MFN2, while upregulation of pro-fission factor DRP1 decreased mean mitochondrial area (Figure S5C). We then monitored the spermatogonial proliferation over 25 days of culture. We found that the spermatogonial morphology and number were not altered upon MFN1, MFN2, or DRP1 overexpression (Figures 4A and S5A). In addition, the SSC marker gene expression of these undifferentiated spermatogonia remained comparable to the level of the empty vector control (Figure 4B). By contrast, upon RA-induced differentiation, enhanced mitochondrial fusion or fission increased the formation of differentiating spermatogonia (Figures 4C and 4D). Consistently, expression of genes that indicate differentiation, including both *Kit* and *Stra8*, was significantly upregulated (Figure 4E), suggesting that enhanced mitochondrial dynamics promote spermatogonial differentiation.

Upregulating MFN1 increases mitochondrial metabolism in differentiating spermatogonia

To explore the potential mechanisms by which accelerated mitochondrial dynamics promote spermatogonial

Figure 3. Reduced mitochondrial dynamics block spermatogonial differentiation

(A) The protein expression of PLZF and DDX4 was analyzed by IHF staining on mouse testes at P14 and P21 with antibodies against PLZF and DDX4, counterstained with DAPI. PLZF+ undifferentiated spermatogonia were not altered upon *Drp1 cKO*.

(B) IHF assays were performed on testicle sections from *Drp1 cKO* mice and $Drp1^{f/+}$ littermates at P21 with antibodies against SYCP3 and DDX4, counterstained with DAPI. Significantly decreased SYCP3+ spermatocytes were detected in *Drp1 cKO* testes. (A and B) Scale bar: 25 μm.

(C) Percentage of CD9+/KIT− undifferentiated spermatogonia and KIT+ differentiating spermatogonia from P14 *Drp1 cKO* and $Drp1^{f/+}$ mice was determined by flow cytometry. Decreased KIT+ differentiating spermatogonia were detected in *Drp1 cKO* mice. $n = 5$.

(D) Undifferentiated and differentiating spermatogonia in the absence (−RA) or presence (+RA) of RA were analyzed via flow cytometry upon knockdown (KD) of the key regulators of mitochondrial dynamics. Decreased KIT+ spermatogonia were detected upon reduced mitochondrial fusion and fission. Representative flow cytometry plots were shown, with graphs below summarizing results from ≥4 independent experiments.

(E) Reduced expression of differentiation markers in differentiating spermatogonia was detected by real-time RT-PCR upon knockdown of key mitochondrial dynamics regulators. $n = 3$. *: $p < 0.05$; **: $p < 0.01$. *n.s.*, no statistical significance. (D and E) SCR, scrambled control shRNA. (C–E) Data were presented as mean ± SEM.

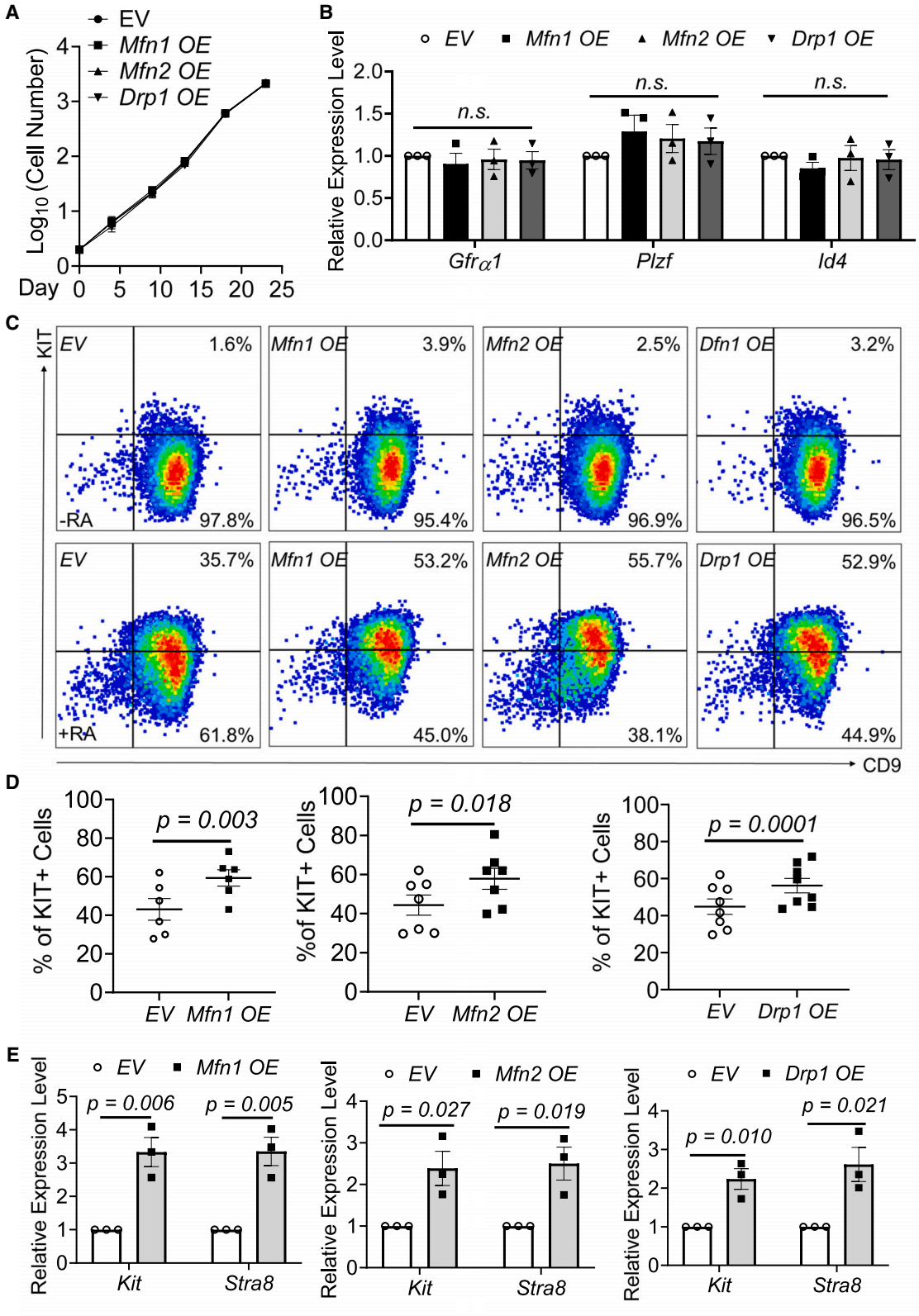

(legend on next page)

differentiation, we measured oxygen consumption rate (OCR) via a Seahorse metabolic analyzer on MFN1-, MFN2-, or DRP1-overexpressing spermatogonia after RA induction for 48 h. We did not observe a noticeable alteration in basal OCR of MFN1- or MFN2-overexpressing differentiating spermatogonia compared to that of the empty vector control (Figures 5A and 5B). A modestly reduced basal OCR was found upon DRP1 overexpression, suggesting reduced OXPHOS when fission increased (Figures 5A and 5B). Interestingly, the maximum mitochondrial respiration, i.e., the change of OCR following the sequential treatment with oligomycin, FCCP (a mitochondrial oxidative phosphorylation uncoupler), and rotenone/antimycin A, was increased in MFN1-overexpressing but not in MFN2- or DRP1-overexpressing spermatogonia, compared to that in empty vector control (Figure 5C), suggesting that MFN1 also regulates mitochondrial metabolism during spermatogonial differentiation.

Increased mitochondrial respiration is usually accompanied by elevated ROS. Indeed, our previous work showed that ROS levels were increased when the bioenergetic preference shifted toward OXPHOS during spermatogonial differentiation (Chen et al., 2020a). ROS can modify protein structures via oxidation or act as signaling molecules to impact a variety of cellular pathways, including stem cell self-renewal (Le Belle et al., 2011; Morimoto et al., 2013). To further investigate whether ROS are required for spermatogonial differentiation, we treated spermatogonia with alpha-lipoic acid (LA), an ROS scavenger, during RA-induced differentiation. We found significantly decreased CD9+/KIT+ differentiating spermatogonia upon LA treatment, compared to the DMSO control, suggesting that spermatogonial differentiation was blocked by reduced ROS (Figure 5D). However, we did not observe significantly altered cellular ROS levels in either undifferentiated or differentiating spermatogonia upon MFN1, MFN2, or DRP1 upregulation (Figure S6A). We further measured the mitochondrial ROS level with MitoSOX, a dye that specifically targets mitochondria in live cells. Oxidation of MitoSOX by mitochondrial ROS generates green fluorescence that can be captured by flow cytometry. No obvious changes in MitoSOX levels were detected across all groups either (Figure 5E), suggesting that mitochondrial dynamics may not promote spermatogonial differentiation via altering the cellular or mitochondrial ROS level.

DRP1 regulates mitochondrial pore opening in spermatogonia

Mitochondrial permeability transition pore (mPTP) is another mitochondrial feature that has been reported in stem cell fate specification. The opening of the mPTP is characterized by a loss of mitochondrial membrane potential (MMP) as well as an increase of cytosolic Ca^{2+}. It has been reported that mPTP opening regulates cell fates, including somatic cell reprogramming toward pluripotent stem cells (Ying et al., 2018). To determine whether mPTP opening is associated with spermatogonial differentiation, we examined mPTP opening using a calcein releasing assay on germ cells from P14 and 8-week-old mouse testes. In this assay, cells are loaded with calcein-AM (acetoxymethyl ester of calcein) and cobalt, the calcein quencher. Intracellular esterases convert calcein-AM to fluorescent calcein. When the mitochondrial membrane is intact, the mitochondrial calcein fluorescence remains high because cobalt cannot cross the mitochondrial membrane. When mPTP opens, cobalt in the cytosol enters the mitochondria and quenches calcein fluorescence. Therefore, low calcein fluorescence represents high mPTP opening. We found that the mPTP opening of KIT+ differentiating spermatogonia was higher than that of CD9+/KIT− undifferentiated spermatogonia from both P14 and adult testes (Figure 6A). Consistently, decreased MMP (Figure 6B) and increased Ca^{2+} levels (Figure 6C) were observed in KIT+ differentiating spermatogonia, compared to the undifferentiated population. Similarly, primarily cultured differentiating spermatogonia upon RA induction exhibited a higher mPTP opening (lower calcein fluorescence) than that of undifferentiated spermatogonia (Figure 6D), supporting our finding that a high mPTP opening is associated with spermatogonial differentiation.

Figure 4. Accelerated mitochondrial dynamics promote spermatogonial differentiation

(A) The cell growth curve of undifferentiated spermatogonia upon overexpressing (OE) key regulators of mitochondrial fusion and fission over a 25-day culture. $n = 3$.

(B) Spermatogonial marker gene expression in four groups from (A) was not altered upon upregulated mitochondrial dynamics regulators, as analyzed by real-time RT-PCR. $n = 3$. *n.s.*, no statistical significance.

(C and D) Flow cytometry analyses on four groups from (A) in the absence (−RA) or presence (+RA) of RA at day 8 post lentiviral infection to enforce the expression of mitochondrial dynamics regulators. Representative flow cytometry dot plots were shown (C), with graphs demonstrating the percentages of KIT+ differentiating spermatogonia from ≥6 independent experiments (D). KIT+ dSPG were increased upon upregulating mitochondrial dynamics regulators.

(E) Expression of marker genes indicating differentiation was increased in spermatogonia with upregulated mitochondrial dynamics regulators following RA treatment for 48 h, as analyzed by real-time RT-PCR. $n = 3$. (A–E) Data are presented as mean ± SEM. EV, empty vector control.

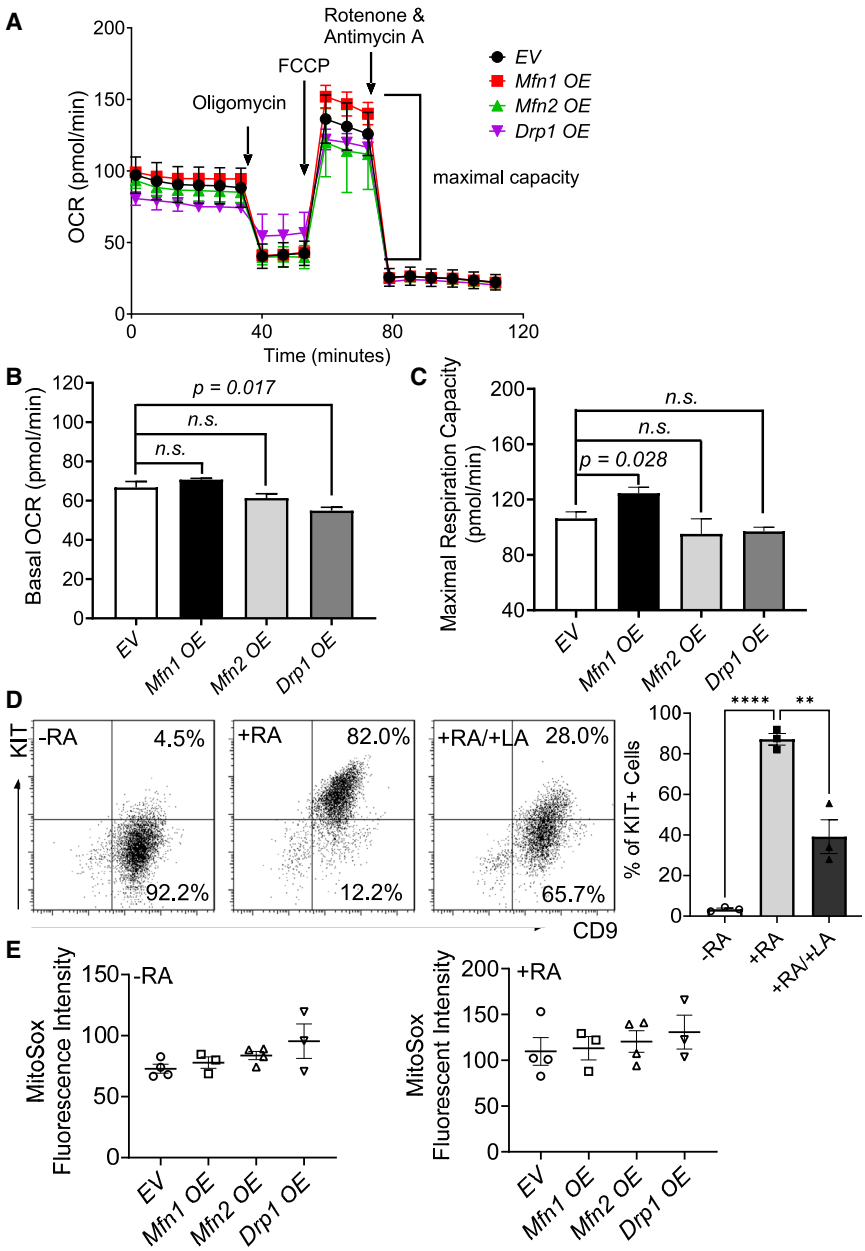

Figure 5. Enhanced MFN1 expression increases mitochondrial metabolism in differentiating spermatogonia

(A–C) Oxygen consumption rate (OCR) (A) was measured in MFN1-, MFN2-, or DRP1-overexpressing spermatogonia after RA treatment for 48 h using a Seahorse XFe96 flux analyzer, with an empty vector as a control. Mitochondrial basal OCR (B) or maximal respiratory capacity (C) was compared across four groups. MFN1 increased maximal respiratory capacity while DRP1 reduced mitochondrial basal OCR.

(D) The formation of KIT+ differentiating spermatogonia upon induction by RA with or without treatment of alpha-lipoic acid (LA) for 48 h was determined using flow cytometry, with DMSO as a vehicle control. Representative flow cytometry dot plots were shown, with the bar graph demonstrating the percentages of KIT+ differentiating spermatogonia. $n = 3$.

(E) Mitochondrial ROS level was measured by flow cytometry on MFN1-, MFN2-, or DRP1-overexpressing spermatogonia without RA treatment (the left panel) and after 48-h RA treatment (the right panel). No statistical significance across all four groups. (A–E) Data are presented as mean ± SEM. $n \geq 3$. *n.s.*, no statistical significance.

To evaluate whether enhanced mitochondrial dynamics regulate mPTP opening during spermatogonial differentiation, we examined the calcein fluorescence intensity by flow cytometry analyses in spermatogonia upon MFN1, MFN2, or DRP1 overexpression. We found comparable mPTP opening levels in undifferentiated spermatogonia across all groups (Figure 6E). Interestingly, increased mPTP opening (with decreased calcein fluorescence) was observed in differentiating spermatogonia upon upregulated DRP1 expression, compared to the empty vector control (Figure 6F, the left panel). By contrast, there were no significant changes in mPTP opening of differentiating spermatogonia across the control, MFN1-, or MFN2-overexpressing groups (Figure 6F, the right panel). We further analyzed the mPTP opening of *Drp1 cKO* mice at P14. We found that calcein fluorescence level did not change in CD9+/KIT− undifferentiated spermatogonia from *Drp1 cKO* mice compared to that of littermate controls, but *Drp1* deficiency in germ cells significantly decreased mPTP opening in KIT+ differentiating spermatogonia (Figure 6G). Taken together, our data reveal that DRP1 specifically regulates mPTP opening during spermatogonial differentiation.

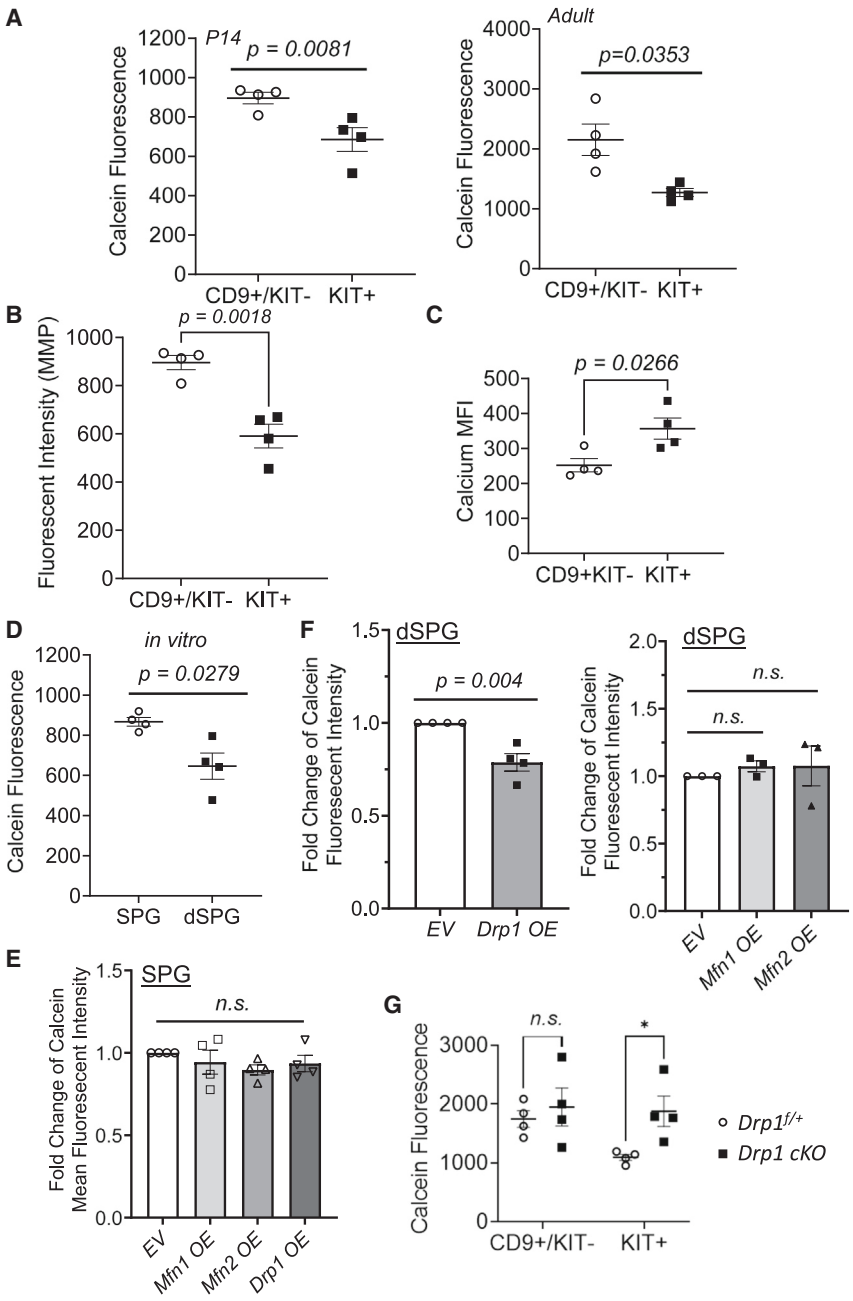

Figure 6. DRP1 regulates mPTP opening during spermatogonial differentiation

(A) The mPTP opening status was measured in CD90+/KIT− undifferentiated and KIT+ differentiating spermatogonia from P14 (the left panel) and 8-week-old mouse testes (the right panel) using flow cytometry. Low calcein fluorescent intensity in KIT+ differentiating spermatogonia represents more mPTP opening.

(B and C) Mitochondrial membrane potential (B) and Ca^{2+} level (C) were analyzed by flow cytometry on the CD90+/KIT− undifferentiated and KIT+ differentiating spermatogonia collected from P14 testes. MFI, mean of fluorescent intensity.

(D) The mPTP opening was examined in cultured undifferentiated spermatogonia and RA-induced differentiating spermatogonia. (B–D) Decreased MMP and increased Ca^{2+} level were detected in differentiating spermatogonia, compared to undifferentiated spermatogonia.

(E and F) The mPTP opening was measured by flow cytometry on CD9+/KIT− undifferentiated spermatogonia (E) and CD9+/KIT+ differentiating spermatogonia upon RA induction (F) in DRP1-, MFN1-, or MFN2-overexpressing (OE) cells. Reduced calcein fluorescent intensity (i.e., more mPTP opening) was detected in dSPG upon DRP1 upregulation.

(G) The mPTP opening was measured by flow cytometry on CD9+/KIT− undifferentiated spermatogonia and CD9+/KIT+ differentiating spermatogonia from *Drp1 cKO* mice and $Drp1^{f/+}$ littermate controls at P14. Increased calcein fluorescent intensity (i.e., reduced mPTP opening) was detected in KIT+ dSPG upon *Drp1* conditional knockout. (A–G) Data are presented as mean ± SEM. $n \geq 3$. *n.s.*, no statistical significance.

DISCUSSION

Mitochondria are increasingly recognized as key players in stem cell differentiation and development. Particularly in spermatogenesis, millions of sperm are continuously generated per day from the adult testes, a process that requires highly coordinated mitochondrial and metabolic activities, but the mechanisms of such coordination are poorly understood. Mitochondria undergo cycles of mitochondrial fission and fusion to exchange their content in order to maintain coordinated responses to various developmental cues, physiological changes, and pathological stress. In this study, we discovered upregulated expression of key pro-fusion GTPases, MFNs (MFN1 & MFN2), OPA1, and pro-fission factors, DRP1, FIS1, and MFF, during spermatogonial differentiation. We further found that mitochondrial fusion and fission are both accelerated. Consistent with this finding, we did not observe significant differences in mitochondrial morphology, quantity, and mtDNA copy number

between undifferentiated spermatogonia and differentiating spermatogonia. Notably, deficiency of either pro-fusion factors (Chen et al., 2020b; Zhang et al., 2016) or pro-fission factor *Drp1* in our current study leads to male infertility, highlighting the importance of properly balanced mitochondrial fusion and fission in supporting germ cell development.

Cellular reliance on mitochondrial metabolism and function varies by cell type and developmental stage. During spermatogonial differentiation, biogenetic preference shifts from glycolysis to mitochondrial respiration to meet increased energy demands. Deficiency of either MFN1 or MFN2, pro-fusion factors, leads to a developmental stage-specific block at the differentiating spermatogonia (Chen et al., 2020b). Similarly, we found that spermatogonial differentiation was specifically blocked in *Drp1 cKO* mice. Although enlarged mitochondria were present in *Drp1*-deficient germ cells at P7 and P14, demonstrating that mitochondrial homeostasis had been disrupted by then, PLZF+ undifferentiated spermatogonia remained intact in *Drp1 cKO* mice at P21. By contrast, decreased formation of KIT+ differentiating spermatogonia accompanied with an elevated percentage of CD9+ undifferentiated spermatogonia was observed in *Drp1* mutant testes, suggesting that spermatogonial differentiation is particularly sensitive to mitochondrial dysfunction and needs to be precisely controlled by concurrently accelerated mitochondrial fusion and fission. Notably, KIT+ differentiating spermatogonia still exist upon knockout of *Mfn1* (Zhang et al., 2016), *Mfn2* (Chen et al., 2020b), or *Drp1*. Functional redundancy of these regulators may compensate for the defects caused by single gene deletion. Future compound gene knockouts may offer a comprehensive understanding of molecular mechanisms underpinning spermatogonial differentiation regulated by mitochondrial dynamics.

Our data further suggest that mitochondrial dynamics may not only play a permissive role in supporting germ cell development but also act as an active driver to promote spermatogonial differentiation. When overexpressed, neither MFNs nor DRP1 affected spermatogonial proliferation, but they significantly enhanced spermatogonial differentiation, compared to the empty vector controls under the same culture conditions. However, upregulated mitochondrial dynamics alone cannot initiate differentiation without RA induction. Thus, it is possible that mitochondrial dynamics prime or facilitate spermatogonial differentiation once RA initiates the process. To understand how upregulated mitochondrial dynamics promote spermatogonial differentiation, we examined mitochondrial metabolic capacity when mitochondrial dynamics regulators were upregulated. This strategy differs from the commonly used gene knockout/knockdown studies, in which deficient mitochondrial dynamics may lead to various changes due to slowed cell proliferation or increased cell death, making it challenging to pinpoint the initial mechanistic contributor. Using this strategy, we found altered mitochondrial metabolic capacity in differentiating spermatogonia upon MFN1 or DRP1 but not MFN2 overexpression. Although we did not observe any obvious altered cristae structure, the overall mitochondrial area or size changed when mitochondrial fusion or fission regulators were upregulated, which may potentially lead to altered levels of OXPHOS. Upregulated mitochondrial metabolism is generally accompanied by increased ROS levels. ROS are not only the byproducts of cellular activities but also the signaling molecules that can regulate a wide variety of physiological processes including SSC self-renewal (Morimoto et al., 2013). Here we observed elevated ROS in differentiating spermatogonia, and ROS scavenger inhibited spermatogonial differentiation, suggesting ROS are required for spermatogonial differentiation. Nevertheless, we did not find evident changes in ROS levels upon upregulated mitochondrial fusion and fission, suggesting that enforced mitochondrial dynamics may not promote spermatogonial differentiation directly via ROS.

Although the three regulators of mitochondrial dynamics that we tested in this study all promote spermatogonial differentiation, they may regulate germ cell fate via different mechanisms (Figure S6C). The mPTP opening is another feature that may change with altered mitochondrial activities to impact cell fate decision (Ying et al., 2018). Our data showed spermatogonial differentiation was associated with increased mPTP opening, while mPTP opening decreased in differentiating spermatogonia upon *Drp1* conditional knockout. Further, enhanced expression of DRP1 but not MFNs promoted mPTP opening, suggesting that DRP1 may function in spermatogonial differentiation by regulating mPTP activity. In support of this notion, a recent study revealed that DRP1 induced the excessive opening of mPTP in vascular smooth muscle cells upon hypoxic injury (Duan et al., 2021).

Other roles of mitochondrial dynamics in spermatogonial differentiation have also been reported. For example, calcium levels may influence mitochondrial respiration and cell fate determination as well. In somatic cells, calcium regulates the activity of rate-limiting enzymes in the TCA cycle such as pyruvate dehydrogenase and α-ketoglutarate dehydrogenase (Robb-Gaspers et al., 1998). In addition, intracellular calcium homeostasis also affects hematopoietic stem cell maintenance (Fukushima et al., 2019). We previously demonstrated that deficiency of MFN2 but not MFN1 disrupted the homeostasis of endoplasmic reticulum (ER) and dysregulated Ca^{2+} levels during spermatogonial

differentiation (Chen et al., 2020b). Subsequently, increased apoptosis and oxidative stress were observed in differentiating spermatogonia from *Mfn2 cKO* mice (Chen et al., 2020b). In this study, we revealed increased level of intracellular calcium in spermatogonia undergoing differentiation, supporting the unique role of MFN2 in regulating calcium homeostasis during spermatogonial differentiation. Notably, although both MFN1 and MFN2 are ubiquitously expressed in various cell types, their expression levels may differ at distinct developmental stages (Khacho et al., 2016). In addition, the exact role of MFN2 in pro-mitofusion or ER functions varies by cell types, and so does their functional reliance on MFN1 or MFN2. For example, MFN2 deficiency in POMC (pro-opiomelanocortin) neurons causes diet-induced obesity due to defects in mitochondrion-ER juxtaposition (Schneeberger et al., 2013), whereas, in agouti-related peptide/Agrp or Purkinje neurons, MFN2 mutations mainly lead to dysfunctional mitofusion (Chen et al., 2007; Schneeberger et al., 2013). Despite the fact that both MFNs are expressed in neurons, only MFN2 mutations result in the human Charcot-Marie-Tooth disease with dysfunctional mitofusion (Züchner et al., 2004). It is yet elusive how MFNs perform these cell-preferential roles.

It remains unclear how increased mitochondrial metabolism or mPTP opening impacts spermatogonial differentiation. In somatic cells, metabolites generated form the TCA cycle not only provide building precursors for the anabolism of nucleotides, lipids, and amino acids but also serve as cofactors (e.g., acetyl-CoA for histone acetylation) for enzymes in epigenetic regulation (Cai et al., 2011). We indeed observed modestly increased acetylated histone 3 upon upregulated mitochondrial dynamics regulators (Figure S6B). The mPTP opening may also play a role in inducing a more "open" chromatin to promote the somatic reprogramming (Ying et al., 2018). Future studies are warranted to investigate whether upregulated mitochondrial metabolism or mPTP opening leads to epigenetic changes that favor spermatogonial differentiation. In addition, we extracted single-cell RNA sequencing data from a recent study (Shami et al., 2020) and compared the expression levels of key mitochondrial dynamics regulators (i.e., *Mfn1*, *Mfn2*, and *Drp1*) in humans, macaques, and mice. Interestingly, we found differentiating spermatogonia have relatively higher expression levels of these mitochondrial regulators than those in undifferentiated spermatogonia also in humans and macaques (Figure S6D), highlighting a conserved mitochondrial regulation across different species. In summary, our current study reveals how mitochondrial functions are maintained by concurrently accelerated and precisely coordinated mitochondrial fusion and fission to support spermatogonial differentiation, a critical and unique event during mammalian reproduction.

EXPERIMENTAL PROCEDURES

Animals

All animal experimental procedures were performed according to the protocols (PROTO202000147 & PROTO202300165) approved by the Institutional Animal Care and Use Committee at Michigan State University. *PhAM* mice (018385) were purchased from The Jackson Laboratory and crossed with *Ddx4-Cre* male mouse (0006954; The Jackson Laboratory) to obtain germ cell-specific expression of mitochondrion-localized Dendra2. Mice with conditional *Drp1* knockout alleles were obtained from Model Animal Research Center (MARC) and maintained in C57BL/6 (000664; The Jackson Laboratory) background. Genotyping PCR primers are listed in Table S2.

Cell culture and primary spermatogonial culture

DBA/2J mouse testes were collected at P6 and dissociated into a single-cell suspension. Undifferentiated spermatogonia were isolated with a fluorescein isothiocyanate (FITC) anti-mouse CD9 antibody (124808; BioLegend) using a Miltenyi Biotec MACS separation kit according to the manufacturer's instruction and cultured in a SSC culture medium, following a published protocol (Kanatsu-Shinohara et al., 2003).

Quantification of the rate of mitochondrial fusion and fission in spermatogonia

Spermatogonia from *PhAM; Ddx4-Cre* mice were seeded in Nunc Lab-Tek II chambered cover glass (155382; Thermo Fisher Scientific) and induced differentiation with 20 nM RA for 48 h. Cells were imaged in the Leica Microsystems TCS SP8 X W.L.L. scanning confocal microscope, following a published protocol (Bertolini et al., 2021) with minor modifications. For acquiring XYZT (XYZ dimensions and time) 4D images, a z stack of 40 slices, a step size of 0.12 mm, and 6-min imaging time were utilized. The images were processed and deconvoluted with the Lighting function of LAS X, the Leica Microsystems software. Mitochondrial volume was quantified in each group over time. The change of mitochondrial volume during the time course is measured compared to the time point before. The fusion and fission events were called when more than 30% in the change of mitochondrial volume occurred.

TEM

TEM on cells and testes was conducted following the published protocols (Chen et al., 2020b; Zhang et al., 2016), with details described in the supplemental experimental procedures.

Flow cytometry

Testis or cultured cells were digested into a single-cell suspension and stained with appropriate dyes or antibodies in the dark: BV421-KIT (561074; BD Biosciences), FITC-CD9 (124808; BioLegend); APC-CD9 (124812; BioLegend), and PE-CD90 (105308; BioLegend). For ROS detection, cells were incubated with 10 μM H2DCFDA (D6883; Sigma), 1 μM MitoSOX Green Reagent (M36005; Invitrogen), or 5 μM CellROX Deep Red Reagent (C10422; Invitrogen) at 37°C for 30 min. The mean

intensity of H2DCFDA dye or Deep Red dye fluorescence was used to calculate ROS levels. For calcein releasing assay, cells were stained with HBSS (14025076; Gibco) containing 10 nM Calcein-AM (14948; Cayman Chemical) and 400 μM $CoCl_2$ (C8661; Sigma) for 15 min at 37°C. To examine MMP or calcium level, cells were stained with 50 nM DiIC1(5) (M34151; Invitrogen) or 4 μM Fluo-4 AM (1041F; ION Biosciences) for 30–45 min at 37°C. Flow cytometers used in this study were BD LSR II, Cytek Aurora, and Attune CytPix.

Histology, IHF staining, and seahorse metabolic OCR assay

Histology, IHF, and OCR were performed according to published protocols (Chen et al., 2020b; Zhang et al., 2016), with detailed description in the supplemental experimental procedures.

Total RNA extraction, western blots, DNA isolation, mtDNA copy number quantification, real-time PCR, plasmid construction, short hairpin RNA (shRNA) knockdown, lentiviral production, concentration, and infection were performed using standard protocols, with antibody information provided in the supplemental experimental procedures. Primer and shRNA sequences are listed in Table S2.

Statistical analysis

All experiments were performed independently at least three times unless specified otherwise. The statistical significance of between-group differences was analyzed with unpaired Student's t test using the GraphPad Prism 8.0 software.

RESOURCE AVAILABILITY

Lead contact

Request for further information and resources should be directed to and fulfilled by Yuan Wang (wangyu81@msu.edu).

Materials availability

All unique and stable reagents generated in this study are available from the lead contact with a completed materials transfer agreement.

Data and code availability

The raw data of mass spectrometry proteomics have been deposited to the ProteomeXchange Consortium via the PRIDE partner repository with the dataset identifier PXD05584 (https://www.ebi.ac.uk/pride/).

ACKNOWLEDGMENTS

We thank Dr. Min Jiang at Westlake University for her help in obtaining *Drp1 cKO* mice. We also thank Drs. Daniel Vocelle and Mathew Bernard at the MSU flow cytometry and Drs. Melinda Frame and Alicia Withrow at the MSU microscopy core facilities for their great services. The Attune CytPix at the MSU flow cytometry core used in this study is supported by the Equipment Grants Program (award #2022-70410-38419) from the U.S. Department of Agriculture (USDA) and National Institute of Food and Agriculture (NIFA). This work was supported by NIH grant R01GM146587 and NSF CAREER grant (IOS2042908).

AUTHOR CONTRIBUTIONS

Z.Z., J.M., H.W., I.A., D.N., and W.C. performed the experiments and analyzed data. Y.W. designed the experiments and analyzed data. Z.Z. and Y.W. wrote the manuscript.

DECLARATION OF INTERESTS

The authors declare no competing interests.

SUPPLEMENTAL INFORMATION

Supplemental information can be found online at https://doi.org/10.1016/j.stemcr.2024.09.006.

Received: March 23, 2024
Revised: September 14, 2024
Accepted: September 16, 2024
Published: October 10, 2024

REFERENCES

Alexander, C., Votruba, M., Pesch, U.E., Thiselton, D.L., Mayer, S., Moore, A., Rodriguez, M., Kellner, U., Leo-Kottler, B., Auburger, G., et al. (2000). OPA1, encoding a dynamin-related GTPase, is mutated in autosomal dominant optic atrophy linked to chromosome 3q28. Nat. Genet. *26*, 211–215.

Anderson, E.L., Baltus, A.E., Roepers-Gajadien, H.L., Hassold, T.J., De Rooij, D.G., Van Pelt, A.M.M., and Page, D.C. (2008). Stra8 and its inducer, retinoic acid, regulate meiotic initiation in both spermatogenesis and oogenesis in mice. Proc. Natl. Acad. Sci. USA *105*, 14976–14980.

Le Belle, J.E., Orozco, N.M., Paucar, A.A., Saxe, J.P., Mottahedeh, J., Pyle, A.D., Wu, H., and Kornblum, H.I. (2011). Proliferative neural stem cells have high endogenous ROS levels that regulate self-renewal and neurogenesis in a PI3K/Akt-dependant manner. Cell Stem Cell *8*, 59–71.

Bertolini, I., Keeney, F., and Altieri, D.C. (2021). Protocol for assessing real-time changes in mitochondrial morphology, fission and fusion events in live cells using confocal microscopy. STAR Protoc. *2*, 100767.

Buaas, F.W., Kirsh, A.L., Sharma, M., McLean, D.J., Morris, J.L., Griswold, M.D., De Rooij, D.G., and Braun, R.E. (2004). Plzf is required in adult male germ cells for stem cell self-renewal. Nat. Genet. *36*, 647–652.

Cai, L., Sutter, B.M., Li, B., and Tu, B.P. (2011). Acetyl-CoA Induces Cell Growth and Proliferation by Promoting the Acetylation of Histones at Growth Genes. Mol. Cell *42*, 426–437.

Chan, D.C. (2006). Dissecting Mitochondrial Fusion. Dev. Cell *11*, 592–594.

Chan, F., Oatley, M.J., Kaucher, A.V., Yang, Q.E., Bieberich, C.J., Shashikant, C.S., and Oatley, J.M. (2014). Functional and molecular features of the Id4+ germline stem cell population in mouse testes. Genes Dev. *28*, 1351–1362.

Chandel, N.S., Maltepe, E., Goldwasser, E., Mathieu, C.E., Simon, M.C., and Schumacker, P.T. (1998). Mitochondrial reactive oxygen species trigger hypoxia-induced transcription. Proc. Natl. Acad. Sci. USA *95*, 11715–11720.

Chen, H., McCaffery, J.M., and Chan, D.C. (2007). Mitochondrial fusion protects against neurodegeneration in the cerebellum. Cell *130*, 548–562.

Chen, W., Zhang, Z., Chang, C., Yang, Z., Wang, P., Fu, H., Wei, X., Chen, E., Tan, S., Huang, W., et al. (2020a). A bioenergetic shift is required for spermatogonial differentiation. Cell Discov. *6*, 56.

Chen, W., Sun, Y., Sun, Q., Zhang, J., Jiang, M., Chang, C., Huang, X., Wang, C., Wang, P., Zhang, Z., et al. (2020b). MFN2 Plays a Distinct Role from MFN1 in Regulating Spermatogonial Differentiation. Stem Cell Rep. *14*, 803–817.

Lo Conte, M., and Carroll, K.S. (2013). The redox biochemistry of protein sulfenylation and sulfinylation. J. Biol. Chem. *288*, 26480–26488.

Duan, C., Kuang, L., Hong, C., Xiang, X., Liu, J., Li, Q., Peng, X., Zhou, Y., Wang, H., Liu, L., and Li, T. (2021). Mitochondrial Drp1 recognizes and induces excessive mPTP opening after hypoxia through BAX-PiC and LRRK2-HK2. Cell Death Dis. *12*, 1050.

Eura, Y., Ishihara, N., Yokota, S., and Mihara, K. (2003). Two mitofusin proteins, mammalian homologues of FZO, with distinct functions are both required for mitochondrial fusion. J. Biochem. *134*, 333–344.

Fukushima, T., Tanaka, Y., Hamey, F.K., Chang, C.H., Oki, T., Asada, S., Hayashi, Y., Fujino, T., Yonezawa, T., Takeda, R., et al. (2019). Discrimination of Dormant and Active Hematopoietic Stem Cells by G0 Marker Reveals Dormancy Regulation by Cytoplasmic Calcium. Cell Rep. *29*, 4144–4158.e7.

Gallardo, T., Shirley, L., John, G.B., and Castrillon, D.H. (2007). Generation of a germ cell-specific mouse transgenic Cre line, Vasa-Cre. Genesis *45*, 413–417.

Guo, J., Grow, E.J., Yi, C., Mlcochova, H., Maher, G.J., Lindskog, C., Murphy, P.J., Wike, C.L., Carrell, D.T., Goriely, A., et al. (2017). Chromatin and Single-Cell RNA-Seq Profiling Reveal Dynamic Signaling and Metabolic Transitions during Human Spermatogonial Stem Cell Development. Cell Stem Cell *21*, 533–546.e6.

Helsel, A.R., Oatley, M.J., and Oatley, J.M. (2017). Glycolysis-Optimized Conditions Enhance Maintenance of Regenerative Integrity in Mouse Spermatogonial Stem Cells during Long-Term Culture. Stem Cell Rep. *8*, 1430–1441.

Hermann, B.P., Cheng, K., Singh, A., Roa-De La Cruz, L., Mutoji, K.N., Chen, I.C., Gildersleeve, H., Lehle, J.D., Mayo, M., Westernströer, B., et al. (2018). The Mammalian Spermatogenesis Single-Cell Transcriptome, from Spermatogonial Stem Cells to Spermatids. Cell Rep. *25*, 1650–1667.e8.

Kanatsu-Shinohara, M., Ogonuki, N., Inoue, K., Miki, H., Ogura, A., Toyokuni, S., and Shinohara, T. (2003). Long-term proliferation in culture and germline transmission of mouse male germline stem cells. Biol. Reprod. *69*, 612–616.

Kanatsu-Shinohara, M., Toyokuni, S., and Shinohara, T. (2004). CD9 Is a Surface Marker on Mouse and Rat Male Germline Stem Cell. Biol. Reprod. *70*, 70–75.

Kanatsu-Shinohara, M., Tanaka, T., Ogonuki, N., Ogura, A., Morimoto, H., Cheng, P.F., Eisenman, R.N., Trumpp, A., and Shinohara, T. (2016). Myc/Mycn-mediated glycolysis enhances mouse spermatogonial stem cell self-renewal. Genes Dev. *30*, 2637–2648.

Khacho, M., Clark, A., Svoboda, D.S., Azzi, J., MacLaurin, J.G., Meghaizel, C., Sesaki, H., Lagace, D.C., Germain, M., Harper, M.E., et al. (2016). Mitochondrial dynamics impacts stem cell identity and fate decisions by regulating a nuclear transcriptional program. Cell Stem Cell *19*, 232–247.

Klose, R.J., Kallin, E.M., and Zhang, Y. (2006). JmjC-domain-containing proteins and histone demethylation. Nat. Rev. Genet. *7*, 715–727.

Kubota, H., Avarbock, M.R., and Brinster, R.L. (2004). Growth factors essential for self-renewal and expansion of mouse spermatogonial stem cells. Proc. Natl. Acad. Sci. USA *101*, 16489–16494.

Lord, T., and Nixon, B. (2020). Metabolic Changes Accompanying Spermatogonial Stem Cell Differentiation. Dev. Cell *52*, 399–411.

Masaki, K., Sakai, M., Kuroki, S., Jo, J.I., Hoshina, K., Fujimori, Y., Oka, K., Amano, T., Yamanaka, T., Tachibana, M., et al. (2018). FGF2 Has Distinct Molecular Functions from GDNF in the Mouse Germline Niche. Stem Cell Rep. *10*, 1782–1792.

Mecklenburg, J.M., and Hermann, B.P. (2016). Mechanisms regulating spermatogonial differentiation. Results Probl. Cell Differ. *58*, 253–287.

Morimoto, H., Iwata, K., Ogonuki, N., Inoue, K., Atsuo, O., Kanatsu-Shinohara, M., Morimoto, T., Yabe-Nishimura, C., and Shinohara, T. (2013). ROS are required for mouse spermatogonial stem cell self-renewal. Cell Stem Cell *12*, 774–786.

Ogawa, T., Dobrinski, I., Avarbock, M.R., and Brinster, R.L. (2000). Transplantation of male germ line stem cells restores fertility in infertile mice. Nat. Med. *6*, 29–34.

Pham, A.H., McCaffery, J.M., and Chan, D.C. (2012). Mouse lines with photo-activatable mitochondria to study mitochondrial dynamics. Genesis *50*, 833–843.

Robb-Gaspers, L.D., Burnett, P., Rutter, G.A., Denton, R.M., Rizzuto, R., and Thomas, A.P. (1998). Integrating cytosolic calcium signals into mitochondrial metabolic responses. EMBO J. *17*, 4987–5000.

Schneeberger, M., Dietrich, M.O., Sebastián, D., Imbernón, M., Castaño, C., Garcia, A., Esteban, Y., Gonzalez-Franquesa, A., Rodríguez, I.C., Bortolozzi, A., et al. (2013). XMitofusin 2 in POMC neurons connects ER stress with leptin resistance and energy imbalance. Cell *155*, 172–187.

Sênos Demarco, R., and Jones, D.L. (2019). Mitochondrial fission regulates germ cell differentiation by suppressing ROS-mediated activation of Epidermal Growth Factor Signaling in the Drosophila larval testis. Sci. Rep. *9*, 19695.

Shami, A.N., Zheng, X., Munyoki, S.K., Ma, Q., Manske, G.L., Green, C.D., Sukhwani, M., Orwig, K.E., Li, J.Z., and Hammoud, S.S. (2020). Single-Cell RNA Sequencing of Human, Macaque, and Mouse Testes Uncovers Conserved and Divergent Features of Mammalian Spermatogenesis. Dev. Cell *54*, 529–547.e12.

Varuzhanyan, G., Ladinsky, M.S., Yamashita, S.I., Abe, M., Sakimura, K., Kanki, T., and Chan, D.C. (2021a). Fis1 ablation in the male germline disrupts mitochondrial morphology and mitophagy, and arrests spermatid maturation. Development *148*, dev199686.

Varuzhanyan, G., Chen, H., Rojansky, R., Ladinsky, M.S., McCaffery, J.M., and Chan, D.C. (2021b). Mitochondrial fission factor

(Mff) is required for organization of the mitochondrial sheath in spermatids. Biochim. Biophys. Acta. Gen. Subj. *1865*, 129845.

Ying, Z., Xiang, G., Zheng, L., Tang, H., Duan, L., Lin, X., Zhao, Q., Chen, K., Wu, Y., Xing, G., et al. (2018). Short-Term Mitochondrial Permeability Transition Pore Opening Modulates Histone Lysine Methylation at the Early Phase of Somatic Cell Reprogramming. Cell Metab. *28*, 935–945.e5.

Zhang, J., Wang, Q., Wang, M., Jiang, M., Wang, Y., Sun, Y., Wang, J., Xie, T., Tang, C., Tang, N., et al. (2016). GASZ and mitofusin-mediated mitochondrial functions are crucial for spermatogenesis. EMBO Rep. *17*, 220–234.

Zhang, Z., Miao, J., and Wang, Y. (2022). Mitochondrial regulation in spermatogenesis. Reproduction *163*, R55–R69.

Züchner, S., Mersiyanova, I.V., Muglia, M., Bissar-Tadmouri, N., Rochelle, J., Dadali, E.L., Zappia, M., Nelis, E., Patitucci, A., Senderek, J., et al. (2004). Mutations in the mitochondrial GTPase mitofusin 2 cause Charcot-Marie-Tooth neuropathy type 2A. Nat. Genet. *36*, 449–451.